J Mater Sci: Mater Med (2009) 20:2385–2394
DOI 10.1007/s10856-009-3811-4

# Formulation and characterization of glass–ceramics based on $Na_2Ca_2Si_3O_9$–$Ca_5(PO_4)_3F$–$Mg_2SiO_4$-system in relation to their biological activity

**H. A. Abo-Mosallam · S. N. Salama · S. M. Salman**

Received: 12 May 2009 / Accepted: 25 June 2009 / Published online: 5 July 2009


**Abstract** Glasses having a chemical composition based on combeite [$Na_2Ca_2Si_3O_9$]–fluoroapatite [$Ca_5(PO_4)_3F$] and forsterite [$Mg_2SiO_4$] system were crystallized through controlled heat-treatment. Two forms of sodium calcium silicate e.g. combeite $Na_2Ca_2Si_3O_9$ and pectolite $Na_2CaSi_3O_8$, were formed together with diopside ($CaMgSi_2O_6$) and monticellite ($CaMgSiO_4$) in addition to fluoroapatite ($Ca_5(PO_4)_3F$) phases by thermal treatment of the glasses. Selected glass–ceramics were exposed to a simulated body fluid solution (SBF) which is close to human plasma for 3 weeks. Energy dispersive X-ray analysis (EDX) and inductive coupled plasma (ICP) analysis confirmed the formation of an apatite layer which indicate bioactivity in the all crystallized sample. A decreasing of surface bioactivity with increasing $Mg_2SiO_4$/$Na_2Ca_2Si_3O_9$ replacement was observed as indicated by the decrease in the amount of apatite layer on the surface of the crystallized specimens. The Vicker's microhardness of the studied glass–ceramic materials are between 5,047 and 6,781 MPa.

## 1 Introduction

Glass–ceramics are polycrystalline materials obtained by the crystallization of high viscous glass-forming melts with appropriate compositions. Their properties basically depend on the kind and percentage of the crystal phases formed and on the composition of the residual glass [1].

Different compositions of bioglasses and glass ceramics are already clinically used as middle ear prostheses, alveolar ridge reconstruction and artificial tooth root materials [2]. It is well known that only a few glasses and glass–ceramics are able to form surface apatite layer similar to the natural bone (Hydroxy Carbonate Apatite, HCA), when they are soaked in a simulated body fluid (SBF) at 37°C. The formation of the apatite layer is believed to be the essential condition for the bonding to the living bone [3]. Bioactive implants should react chemically with body fluids in a manner compatible with the repair process of the tissues. First, an amorphous calcium phosphate (a-CaP) rich layer is formed on the surface of the bioactive materials when implanted. The initial a-CaP crystallizes to hydroxyl carbonate apatite (HCA) analogous to that present in bones. The HCA crystals, together with collagen fibres form the bonding layer [4].

The first bioglass, Bioglass 45S5, was developed by Hench. It represents the simplest formulation of all known compositions: 46.1% $SiO_2$, 26.9% CaO, 24.2% $Na_2O$, and 2.6% $P_2O_5$ in mole percent. This glass is the most studied, bioactive, and the most used up to now [5]. The well-known bioactive glass 45S5 shows sodium–calcium–silicate type crystals at devitrification. Most often the crystals have been reported as $Na_2Ca_2Si_3O_9$ [6].

The bioactivity reaction stages of this material, which predominately forms the crystalline phase $Na_2Ca_2Si_3O_9$ when heated, are similar to that of amorphous 45S5 bioactive glass [7]. Salman et al. [8] reported that, the sodium calcium silicate ($Na_2Ca_2Si_3O_9$) phase has higher bioactive index than fluoroapatite. Clupper et al. [9] studied the function of the heat treatment processing conditions on the strength and toughness of 45S5 Bioglass. They reported that, the strength and toughness of bioactive glass ceramic samples approached that of natural cortical bone.

A part of the glass–ceramics developed in the last years for biomedical applications is based on the CaO–MgO–$P_2O_5$–$SiO_2$ system. Glasses and glass ceramics consisting

H. A. Abo-Mosallam (✉) · S. N. Salama · S. M. Salman
Glass Research Department, National Research Centre,
El-Behoos St. Dokki, Cairo, Egypt
e-mail: abomosallam@yahoo.com.au

of this system show bioactivity and bonds to living bone after implantation [10]. Kokubo et al. [11] presented a new type of apatite containing glass ceramic for the system MgO 4.6%, CaO 44.9%, $SiO_2$ 34.2%, $P_2O_5$ 16.3%, $CaF_2$ 0.5% which can form a tight chemical bond with bones and has a high mechanical strength.

Salinas et al. [12] manufactured bioactive glass–ceramics from $3CaO–P_2O_5–CaO{\cdot}SiO_2–CaMgSi_2O_6$ ternary system. Salama et al. [13] prepared a new bioglass–ceramics based on the stoichiometric compositions of 75 $CaMgSi_2O_6$–25 $Ca_5(PO_4)_3F$, with minor amounts of $Na_2O$. Glass–ceramic materials based on diopside [$CaMgSi_2O_6$]–wollastonite [$CaSiO_3$]–fluoroapatite [$Ca_5(PO_4)_3F$]–sodium silicate [$Na_2SiO_3$] system were successfully prepared and examined in vitro to be suitable for restorative dental and bone implant materials [8].

The aim of the present work was to study the crystallization characteristics of glasses based on various content of the stoichiometric compositions of combeite [$Na_2Ca_2Si_3O_9$]–fluoroapatite [$Ca_5(PO_4)_3F$]–foresterite [$Mg_2SiO_4$] system and determine the bioactivity behaviour by using (SBF) solution and microhardness of crystalline materials.

## 2 Experimental

### 2.1 Batch composition and glass preparation

The glass compositions were calculated to give different proportions of combeite [$Na_2Ca_2Si_3O_9$]–fluoroapatite [$Ca_5(PO_4)_3F$] and forsterite [$Mg_2SiO_4$]. The calculated weight percentages of forsterite gradually increased from 5 to 25% at the expense of combeite with constant contents of fluoroapatite phase. The chemical compositions of the prepared glasses are given in Table 1.

Appropriate weight of reagent grade powders of $CaCO_3$, $SiO_2$ (quartz), MgO, $P_2O_5$, $CaF_2$, and $Na_2CO_3$, were thoroughly mixed and melted in Pt/Rh crucible in an electric furnace with SiC heating elements at 1,300–1,375°C for 3 h. Melting was continued until clear homogeneous melt was obtained; this was achieved by swirling the melt several times at about 30-min intervals. The melt was cast into rods and as buttons, which were then properly annealed in a muffle furnace at 550°C to minimize the strain.

### 2.2 Differential scanning calorimetry (DSC)

The controlled heat-treatment parameters of the glasses were determined by the differential scanning calorimetry using a Stanton Redcroft DSC 1500 (Rheometric Scientific, Epsom UK). The crucibles used were matched pairs made of Platinum–Rhodium alloy. Alumina was used as the reference material. Runs were performed in air at a heating rate of 10°C $min^{-1}$.

### 2.3 Materials investigation

Identification of the crystal phases precipitating due to the course of crystallization was conducted by X-ray diffraction (XRD) analysis of the powdered glass–ceramic samples. The X-ray diffraction patterns were obtained by using Phillips powder diffractometer (Phillips Xpert diffractometer, Phillips Eindhoven NL) with Cu Kα X-rays. The reference data for the interpretation of the X-ray diffraction patterns were obtained from ASTM X-ray diffraction card files. The crystallization characteristics and internal microstructures of fractured surfaces of the crystalline samples, after etched by 1% ($HNO_3$–HF) solution and coated with gold spray, were examined by using scanning electron microscopy (SEM). Representative electron micrographs were obtained by using Jeol, JXA-840 Electron Probe Microanalyzer.

### 2.4 Properties

#### *2.4.1 Bioactivity (vitro test)*

In vitro bioactivity tests all the specimens were carried out in polyethylene containers soaking the samples at 37 ± 0.5°C, for 7, 14 and 21 days in 50 ml of Tris-buffered simulated body fluid (SBF) solution, whose composition is shown in Table 2. Specimens were mounted vertically in a special polyethylene scaffold to avoid deposition by gravity. The SBF was prepared by dissolving

**Table 1** The composition of the investigated glass

| Glass no. | Theoretical phase constituents (wt%) | | | Oxide constitutions (wt%) | | | | | |
|---|---|---|---|---|---|---|---|---|---|
| | Comb | FA | FO | $Na_2O$ | CaO | $SiO_2$ | MgO | $P_2O_5$ | $CaF_2$ |
| $G_1$ | 75 | 25 | – | 13.1 | 36.26 | 38.15 | – | 10.55 | 1.94 |
| $G_2$ | 70 | 25 | 5 | 12.24 | 34.67 | 37.74 | 2.86 | 10.55 | 1.94 |
| $G_3$ | 65 | 25 | 10 | 11.37 | 33.08 | 37.33 | 5.73 | 10.55 | 1.94 |
| $G_4$ | 60 | 25 | 15 | 10.49 | 31.5 | 36.93 | 8.59 | 10.55 | 1.94 |
| $G_5$ | 55 | 25 | 20 | 9.62 | 29.92 | 36.51 | 11.46 | 10.55 | 1.94 |
| $G_6$ | 50 | 25 | 25 | 8.75 | 28.34 | 36.1 | 14.32 | 10.55 | 1.94 |

*Comb* combeite $Na_2Ca_2Si_3O_9$, *FA* Fluorapatite[$Ca_5(PO_4)_3F$], *FO* Forsterite [$Mg_2SiO_4$]

**Table 2** Ionic concentrations (mM) in the simulated body fluid (SBF) and human Plasma

| Occurrence | Ions concentrations (mM) | | | | | | | |
|---|---|---|---|---|---|---|---|---|
| | $Na^+$ | $K^+$ | $Mg^{2+}$ | $Ca^{2+}$ | $Cl^-$ | $HCO^-$ | $HPO_4^{2-}$ | $SO^{4-}$ |
| Human plasma | 142.0 | 5.0 | 1.5 | 2.5 | 103.0 | 27.0 | 1.0 | 0.5 |
| (SBF) | 142.0 | 5.0 | 1.5 | 2.5 | 147.8 | 4.2 | 1.0 | 0.5 |

reagent grade NaCl, $NaHCO_3$, KCl, $K_2HPO_4{\cdot}3H_2O$, $MgCl_2{\cdot}6H_2O$, $CaCl_2$, and $Na_2SO_4$ into deionized water. The solution was buffered to pH 7.4 with Tris-(hydroxymethyl)–aminomethan $[(CH_2OH)_3{\cdot}CNH_3]$ and hydrochloric acid. Surface modifications of the materials were studied by scanning electron microscope with energy dispersive X-ray analysis (SEM-EDX) Model INCA x-sight. The variation of ion concentrations in the (SBF) solution after soaking the sample was monitored by using inductive coupled plasma (ICP) Model (Jobian Yvon Horiba Ultima 2000). The changes in pH of the SBF solution as a function of time were monitored using a pH meter (Hanna 8417). Each pH value reported is mean of four measurements performed at each recording time.

### *2.4.2 Microhardness*

The microhardness of the crystallized samples was measured by using Vicker's microhardness indenter (Model Zwick/ZHV1-m microhardness tester). The specimens were cut using a low speed diamond saw, dry ground and polished carefully to obtain smooth and flat parallel surfaces of glass–ceramic samples before indentation testing. At least six indentation readings were made and measured for each sample. Testing was made using a load of 100 g; loading time was fixed for all the crystalline samples (15 s). The measurements were carried out under normal atmospheric conditions. The microhardness values are converted from $kg/mm^2$ to MPa by multiplying with a constant value 9.8.

## 3 Results

### 3.1 Crystallization characteristics

The DSC data (Fig. 1) of the studied glasses showed endothermic effects in the 606–629°C temperature range, at which the atoms seems to be arranged themselves in preliminary structural elements preceding the nucleation. Various exothermic effects in the 775–831°C temperature range, indicating crystallization in the glasses, are also recorded. However, the heat-treatment was carried out

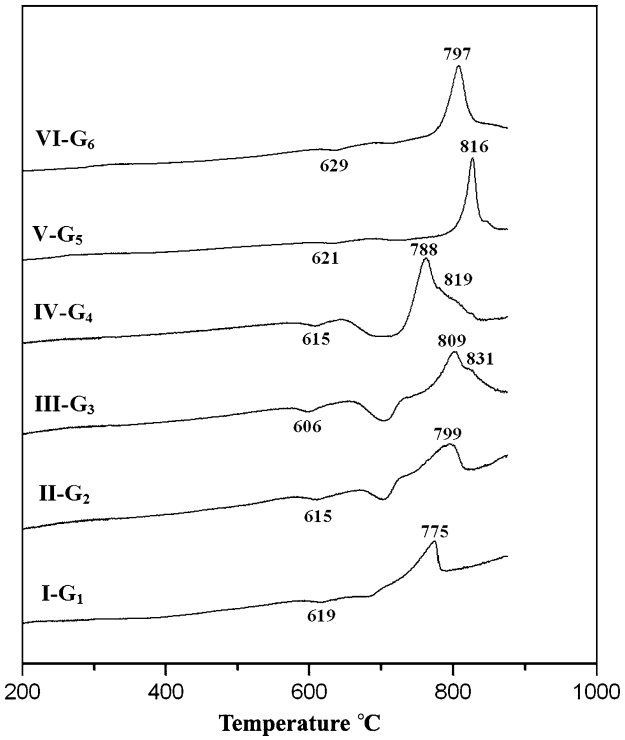


**Fig. 1** DSC data of the glasses

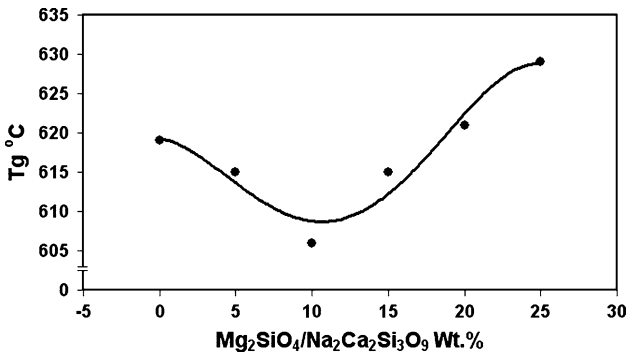


**Fig. 2** $T_g$ trend for the glasses with increasing $Mg_2SiO_4/Na_2Ca_2Si_3O_9$ replacement

using the higher exothermic peak temperature to attain the most stable phases in the crystalline glasses ($G_1$–$G_6$). The plot of the glass transition temperatures ($T_g$) against the $Mg_2SiO_4/Na_2Ca_2Si_3O_9$ replacement was shown in Fig. 2.

The X-ray diffraction analysis (Fig. 3, Pattern I) revealed that the base glass $G_1$ thermally heated at 620°C/5 h–775°C/10 h, crystallized into sodium calcium silicate [combeite–$Na_2Ca_2Si_3O_9$] (major lines 3.30, 3.05, 2.67, 2.19, 2.18, 2.15, 1.80, 1.65, 1.60, Card No. 22-1455) as a major phase and fluoroapatite (lines 3.45, 2.81, 2.77, 2.71, 2.13, 1.82, 1.75, 1.72, Card No. 15-876) as a secondary phase. On partial replacement of $Mg_2SiO_4$ instead of $Na_2Ca_2Si_3O_9$ in the glasses, diopside phase (major lines 3.31, 3.21, 2.98, 2.94, 2.88, Card No. 19-239) was detected

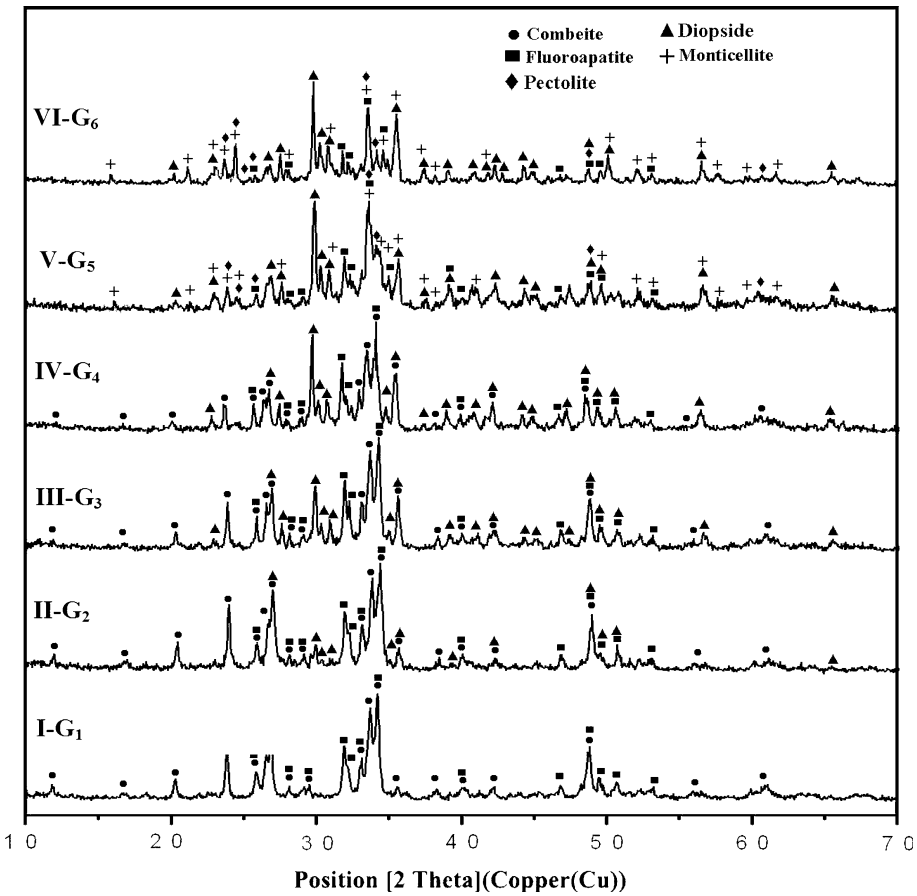


**Fig. 3** XRD analysis of crystallized glasses

with the combeite and fluoroapatite phases. However, the amount of diopside phase was increased at the expense of combeite with the $Mg_2SiO_4/Na_2Ca_2Si_3O_9$ replacement as indicated from XRD analysis of $G_2$, $G_3$ and $G_4$ samples (Fig. 3, Patterns II, III and IV, respectively).

The increase of $Mg_2SiO_4$ at the expense of $Na_2Ca_2Si_3O_9$ in glasses $G_5$ and $G_6$ heat-treated at 620°C/5 h–816°C/10 h and 630°C/5 h–800°C/10 h, respectively, led to the formation of pectolite–$Na_2CaSi_3O_8$ phase (major lines 3.75, 3.38, 3.33, 2.86, 2.63 Card No. 12-671) and monticellite ($CaMgSiO_4$) phase (major lines 4.18, 3.62, 2.98, 2.93, 2.66, Card No. 19-240) together with diopside and fluoroapatite phases (Fig. 3, Patterns V and VI).

SEM micrographs of the fractured surfaces, Fig. 4a–c, show the effect of increasing $Mg_2SiO_4$ at the expense of $Na_2Ca_2Si_3O_9$ on the microstructure of the glass–ceramic samples ($G_1$, $G_4$ and $G_6$). The SEM micrograph (Fig. 4a) of the fractured surface of the crystallized glass $G_1$ showed tiny aggregate microstructure. Figure (4b) of sample $G_4$ shows volume crystallization of oriented fibrous-like growths. However, volume crystallization of denderite-like growths was formed in the crystalline sample $G_6$ (with high amount of $Mg_2SiO_4$, 25 wt%), Fig. 4c.

## 3.2 Properties

### *3.2.1 Bioactivity (vitro test)*

Figure 5 correlates the elemental concentrations of Ca, Mg, Si, and P in SBF solution with the immersion time by using ICP technique. All ion concentrations increased in the early stages of soaking in SBF solution (after 7 days). For each glass–ceramic sample silicon and magnesium concentrations were gradually increased while calcium and phosphorous concentrations were decreased with immersion time. The depletion in calcium and phosphorous ions indicates that they are precipitating on the material surfaces. The higher rates of change occur for the free-MgO sample ($G_1$); therefore, this glass–ceramic sample presents a higher surface reactivity.

Figure 6 shows the changes in pH after various time periods of in vitro dissolution. It can be clearly noticed that the pH value of the SBF solution in all samples decreases with $Mg_2SiO_4$-content in the glass, for each soaking time. For each glass–ceramic composition the pH value gradually increases with soaking time when compared to the pH value of the initial SBF solution.

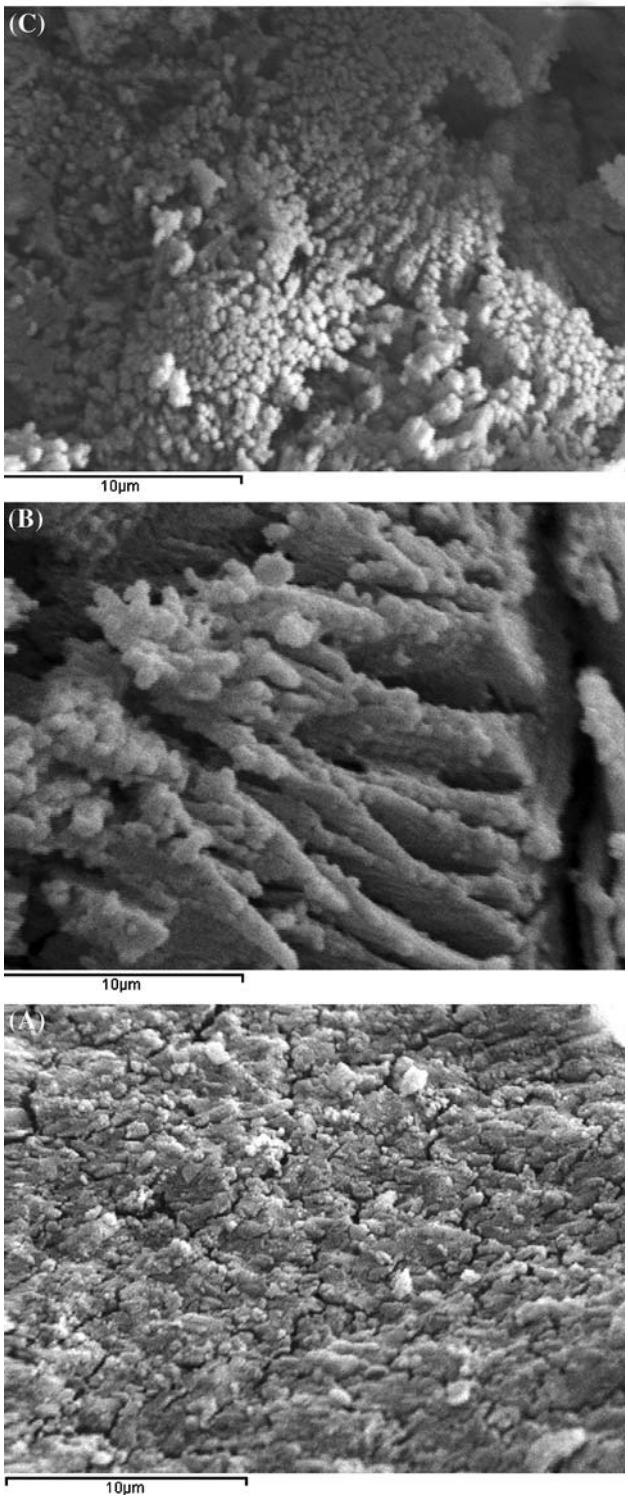


**Fig. 4** **a** SEM micrograph of fracture surface of glass–ceramic $G_1$, **b** SEM micrograph of fracture surface of glass–ceramic $G_4$ and **c** SEM micrograph of fracture surface of glass–ceramic $G_6$

Figures 7, 8, and 9 showed SEM and EDX spectra of the selected glass–ceramic samples before and after soaking in SBF solution. Figures 7a, 8a, and 9a showed the micrographs of the crystallized samples (i.e. $G_1$, $G_4$ and $G_6$, respectively) after the immersion in the simulated body fluid (SBF) for 21 days at 37°C. The scanning electron micrographs (Figs. 7a, 8a, and 9a) of the crystalline samples show that surface layers are formed with different shapes which are assumed to be due to the formation of apatite phase.

Figures 7b, 8b, and 9b show a comparison of the EDX spectra of glass–ceramic surfaces before and after soaking in SBF solution. The EDX spectra (Fig. 7b) collected from the crystallized base glass sample ($G_1$) before immersion in SBF solution recorded the presence of Ca, Na, Si, and P elements with different ratios. After immersion in the SBF solution for 21 days, the EDX spectra revealed that, layers rich in Ca and P were detected at the surface of the sample.

Figures 8b and 9b represent the EDX spectra of the surfaces of glass–ceramic samples $G_4$ and $G_6$, respectively (before and after immersion in SBF solution). The presence of Ca, Na, Mg, Si, and P elements on the surface of the studied glass–ceramics were recorded before immersion. The addition of $Mg_2SiO_4$ at the expense of $Na_2Ca_2Si_3O_9$ with various ratios, i.e. $G_4$ and $G_6$ led to increase the intensity of Mg peak at the expense of Na and Ca peaks (Figs. 8b, 9b). The EDX spectra of the surfaces of the samples after immersion in the SBF solution for 21 days revealed that, layers rich in Ca and P, but poor or rare in Si, Mg and Na were detected on the surfaces of the samples.

### *3.2.2 Microhardness*

The Vicker's microhardness values of the investigated glass–ceramic materials were summarized in Table 2. The data are also graphically represented in Fig. 10 from which it could be seen that, the increase of $Mg_2SiO_4$ at the expense of $Na_2Ca_2Si_3O_9$ in the base glass ($G_1$) generally led to increase the microhardness values of the crystalline samples (i.e. $G_2$–$G_6$). The hardness value of sample $G_1$ (free of $Mg_2SiO_4$) exhibits the lowest value (5,047 MPa) (Table 3, Fig. 10).

## 4 Discussion

The glass transition temperature ($T_g$) and crystallization temperature ($T_c$) were studied to determine the effect of the substitution of $Na_2Ca_2Si_3O_9$ with $Mg_2SiO_4$ on the crystallization temperatures of the glasses. The present results revealed that the endothermic temperatures ($T_g$) were shifted to lower values by adding $Mg_2SiO_4$ instead of $Na_2Ca_2Si_3O_9$, $G_1$–$G_3$ glasses. This could be attributed on the basis that MgO seemed to be incorporated in the glass structure as a network former. Magnesium oxide has an intermediate behaviour with respect to the glass formation and has been shown to have both six and four oxygen coordination [14]. In

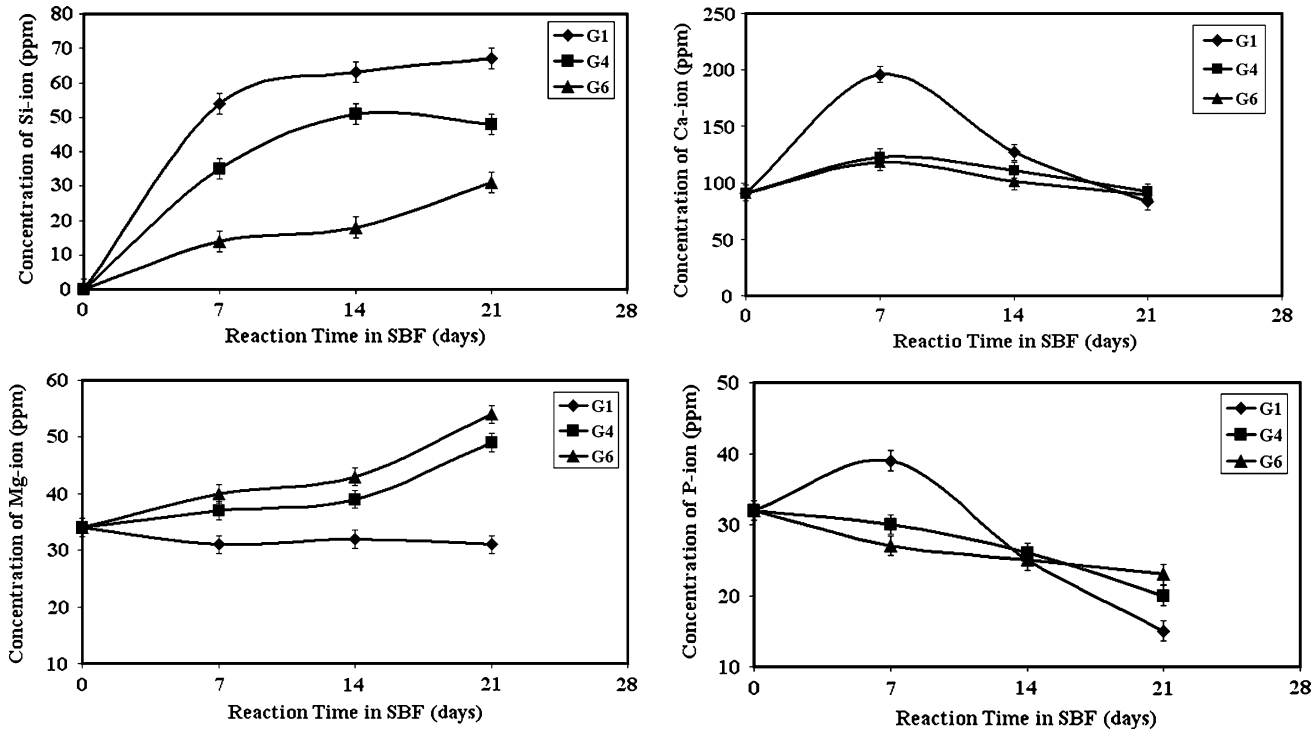


**Fig. 5** Ion concentrations in SBF solution after immersion of glass–ceramic samples for 7, 14 and 21 days

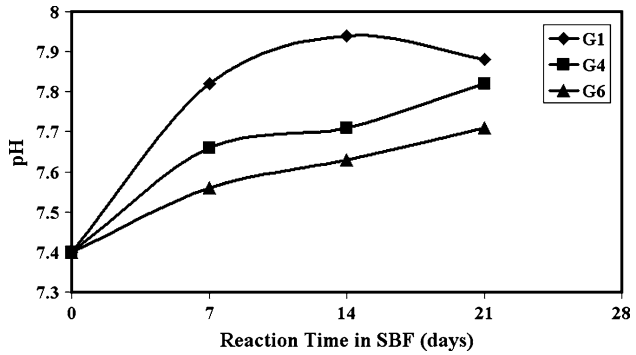


**Fig. 6** pH of SBF solution after immersion of glass–ceramic samples for 7, 14 and 21 days

fact, the formation of a weaker bond between the oxygens and the magnesium with respect to a Si–O bond, (3.35 eV vs. 8.10 eV) could result in a reduction of the $T_g$ as less energy is required to break the bonds [15].

The increase of the $T_g$ in glass samples $G_4$–$G_6$ may be explained on the basis that before the minimum $T_g$ value (Fig. 2, i.e. $G_3$ with 10 wt% $Mg_2SiO_4$), mainly calcium charge balance the magnesium entering the network of the glass and sodium is acting like a modifier and is not involve in this process so a relatively disrupted network could be occurred. While after the minimum $T_g$ value, in Fig. 2, the calcium is not enough to charge balancing the magnesium entering the network of the glasses, may be because of its lower concentration in the glasses, so sodium will charge balance the magnesium entering the network of the glass. Thus a less disrupted network and consequently a higher $T_g$ is found [15].

Investigation of the glass–ceramic materials by X-ray diffraction analysis revealed that predominant combeite and fluoroapatite phases were crystallized from the base glass $G_1$. Sodium calcium silicate, identified as the major phase together with fluoroapatite, were also identified by Li et al. [16], on the crystallization of bioactive glass containing (in wt%) $SiO_2$ 48, $P_2O_5$ 9.5, $Na_20$ 20 and CaO 22.5.

Mineralogically, the addition of $Mg_2SiO_4$ at the expense of $Na_2Ca_2Si_3O_9$ in the glasses $G_2$–$G_4$, diopside ($CaMgSi_2O_6$) was developed at the expense of combeite phase ($Na_2Ca_2Si_3O_9$) as indicated from the decrease of the peak intensities of XRD of combeite phase. Diopside–$CaMgSi_2O_6$ is one of the most important mineral phases of the pyroxene family [17]. Pyroxenes consist of a group of minerals of variable composition, which crystallized fairly readily. They are closely related in crystallographic and other physical properties, as well as, in chemical composition [17]. Nonami, [18] reported that, the chain silicate minerals such as diopside have been synthetically prepared for use as bioactive ceramic materials.

On increasing $Mg_2SiO_4$ instead of $Na_2Ca_2Si_3O_9$, i.e. glasses $G_5$ and $G_6$, pectolite [$Na_2CaSi_3O_8$] and monticellite ($CaMgSiO_4$) phases were developed and monticellite phase increased gradually with the $Mg_2SiO_4$/$Na_2Ca_2Si_3O_9$ replacements. Monticellite, $CaMgSiO_4$, is part of the

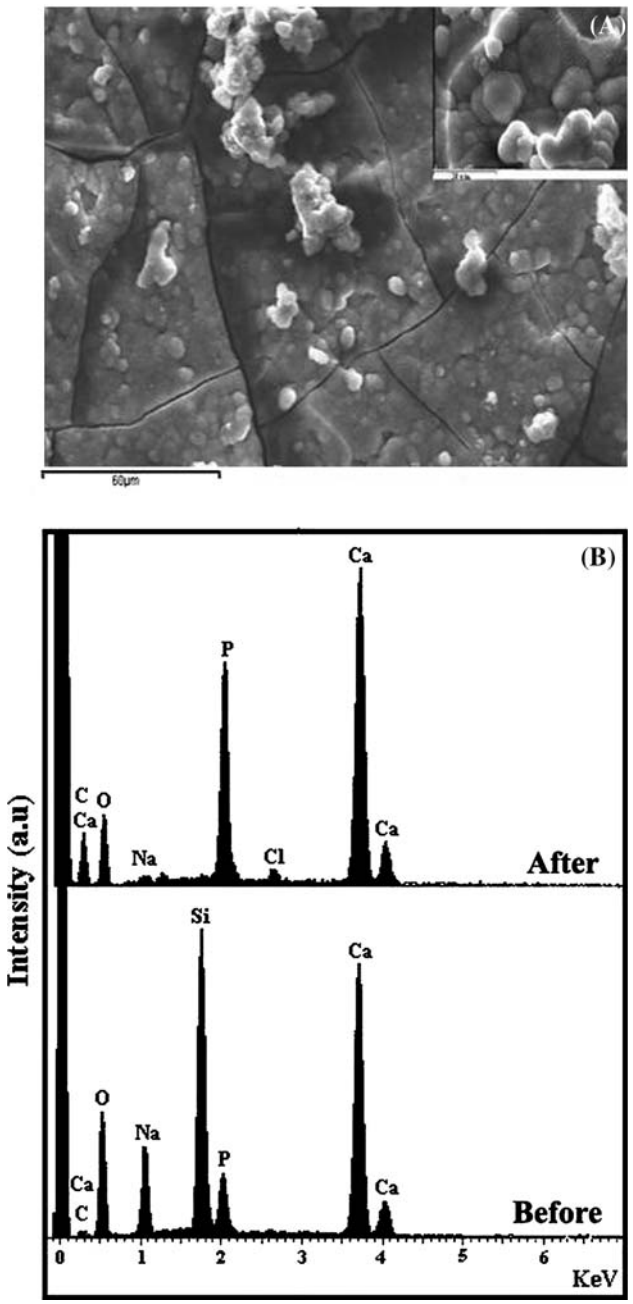


**Fig. 7** **a** SEM micrograph of the glass–ceramic surface of specimen $G_1$ after the immersion in the (SBF) solution, **b** EDX of the glass–ceramic surface of specimen $G_1$ before and after the immersion in the (SBF) solution

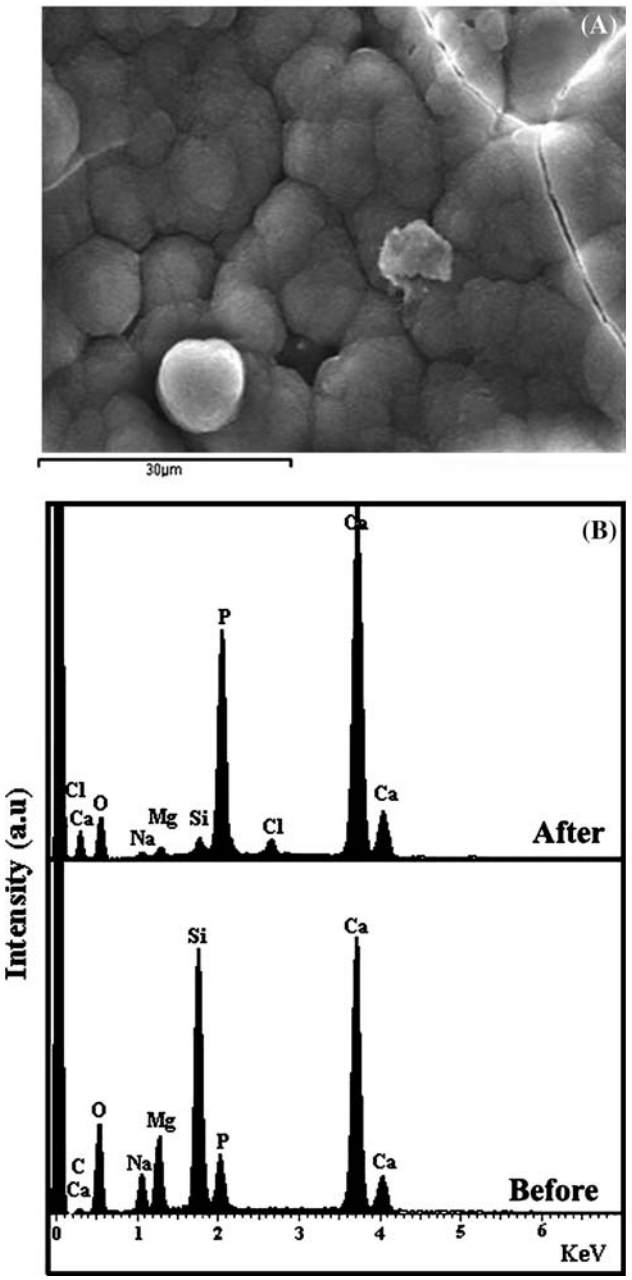


**Fig. 8** **a** SEM micrograph of the glass–ceramic surface of specimen $G_4$ after the immersion in the (SBF) solution, **b** EDX of the glass–ceramic surface of specimen $G_4$ before and after the immersion in the (SBF) solution

olivine. Ricker and Osborn [19] reported that the olivine solid solution extends from the $CaMgSiO_4$ composition towards $Mg_2SiO_4$, but not towards merwinite $Ca_3MgSi_2O_8$.

In biomaterials research, the in vitro studies involving dissolution experiments in solutions similar in composition to those present inside the human body (e.g. simulated body fluid, SBF have now been recognized as preliminary screening tests on new candidate implant materials [20]. The bio-characteristic of bioactive glasses and bioactive ceramics is a time-dependent and kinetic modification of the surface that occurs upon implantation. The surface forms a biologically active hydroxycarbonate apatite (HCA) phase that forms on bioactive implants that are chemically and structurally equivalent to the mineral phase in the bone. It means equivalence that is responsible for interfacial bonding [21]. The surface change of bioactive glass–ceramics in vivo and in vitro is more complex than that of single phase bioactive glasses by virtue of their multiphase [16]. The in vitro

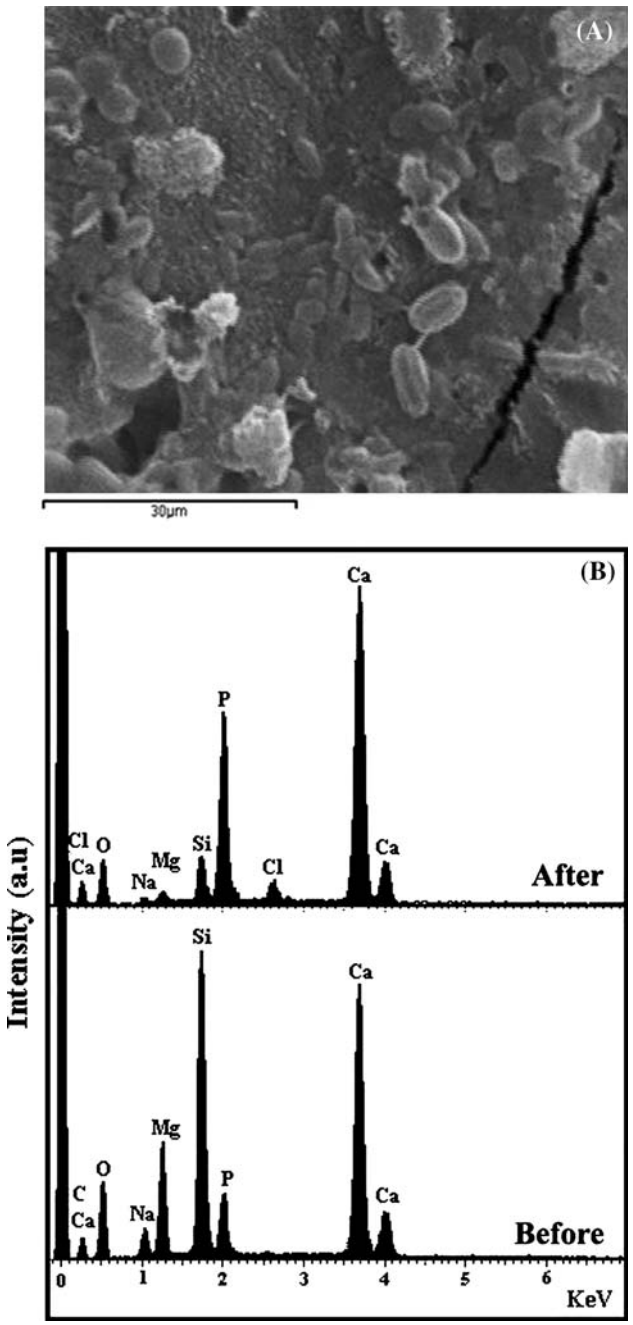


**Fig. 9** **a** SEM micrograph of the glass–ceramic surface of specimen $G_6$ after the immersion in the (SBF) solution, **b** EDX of the glass–ceramic surface of specimen $G_6$ before and after the immersion in the (SBF) solution

study in the SBF solution of the selected studied glass–ceramic samples revealed that each one showed different bioactivity behaviour in vitro-test.

A quantitative analysis of the ions in the solution after in vitro tests is very useful to complement the understanding of surface kinetic reactions in bioactive materials [22]. The highly bioactive material, 45S5 Bioglass®, was used as the standard for comparison with the model glasses and glass–ceramics.

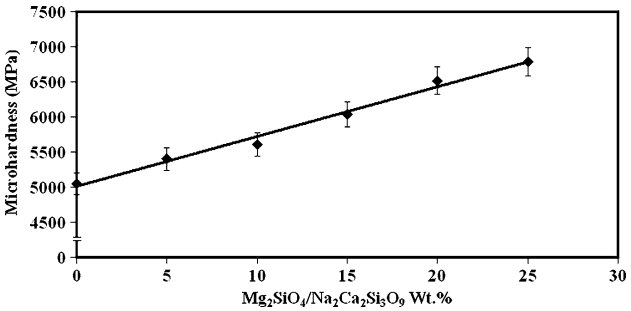


**Fig. 10** Microhardness values of the crystallized glasses

In the early stage of immersion of the glass–ceramic samples, the concentration of all ions were increased in the SBF solution. Alkali and alkaline earth ions are released very rapidly in the early stage of immersion (after 7 days, Fig. 5) to the SBF solution and this led to increase its pH value. The first stage of the reaction kinetics of bioglass and bioglass ceramics is the rapid exchange of ions of $Na^+$ or $K^+$ with $H^+$ or $H_3O^+$ from solution. This alkalinity results in a local rise of pH value [2]. The increase in pH actually signifies for the reduction in the concentration of $H^+$ due to the replacement of metal ions in the glass and subsequent production of $OH^-$ ions, due to breaking of siloxane bond [20]. In general the extraction rate of alkaline-earth ions decreases with decreasing ionic radius [23] and so reduction in the pH value of Mg-containing glass–ceramics were expected as the $Mg_2SiO_4$ content increases. Figures 5 and 6 show that increasing $Mg_2SiO_4$ content in the glasses decreasing the dissolution of the glass–ceramic materials, with a corresponding decrease in pH value.

The depletion of Ca and P concentrations and the increase of the silicon and magnesium in the SBF solution with the immersion time was observed, these ion concentrations change may be associated with the apatite layer formation. The decrease in the concentration of Ca and P ions in the SBF solution per-immersion time indicated that there was apatite layer formed on the surfaces of the glass–ceramic samples [24]. Peitl et al. [2] reported that the decrease in calcium and phosphorous ion concentrations in the SBF solution indicates the formation, crystallization and growth of the $CaO–P_2O_5$ rich layer.

The silicon release from the glass–ceramic significantly decreased with $Mg_2SiO_4$ addition. This indicates that the reaction between the glass–ceramic samples and SBF solution was suppressed and formation of apatite layer was also suppressed as seen in the sample $G_4$ and $G_6$. This may be attributed to the chemical durability of the glass–ceramic samples are improved by the addition of $Mg_2SiO_4$. The bioactivity behaviour of a glass or a glass–ceramic depends on its composition, but is mainly determined by surface chemical reactivity. The higher the solubility of the various oxides of the material in the host medium, the easier the

**Table 3** The crystalline phases developed and microhardness values of the investigated glass–ceramics (i.e. $G_1$–$G_6$)

| Glass no. | Heat-treatment (°C/h) | Microhardness (MPa) | Developed phases |
|---|---|---|---|
| $G_1$ | 620/5 h–775/10 h | 5,047 | Comb. + FA |
| $G_2$ | 715/5 h–800/10 h | 5,399 | Comb. + FA + Diop (minor) |
| $G_3$ | 605/5 h–810/10 h | 5,605 | Comb. + FA + Diop (increased) |
| $G_4$ | 615/5 h–790/10 h | 6,036 | Comb. + Diop + FA + Mont (minor) |
| $G_5$ | 620/5 h–815/10 h | 6,517 | Diop + Pect. + FA + Mont (little) |
| $G_6$ | 630/5 h–800/10 h | 6,781 | Diop + Mont (increased) + Pect. + FA |

*Comb* combeite [$Na_2Ca_2Si_3O_9$], *FA* Fluorapatite [$Ca_5(PO_4)_3F$], *Diop* Diopside [$CaMgSi_2O_6$], *Mont* monticellite [$CaMgSiO_4$], *Pect.* Pectolite [$Na_2CaSi_3O_8$]

precipitation of the surface layer responsible for bioactivity [25].

Further evidence to confirm the presence of apatite layers on the surfaces of glass–ceramic samples with different magnitude, was sought by using the EDX technique before and after the soaking in the SBF solution. Figure 7b shows the EDX trace from the surface of the base glass–ceramic $G_1$ (containing combeite and fluoroapatite phases) before soaking in the SBF solution indicating the presence of Ca, Na, Si and P. EDX spectra from the same sample after immersion in the SBF solution for 21 days revealed that significant peaks for Ca and P were detected due to the formation of the apatite layer on the surface. Peitl et al. [2] demonstrated that in vitro tests fully crystallized $Na_2Ca_2Si_3O_9$ glass–ceramic are much more bioactive than any commercial bioactive ceramics or other glass–ceramic. Chen et al. [26] succeeded in the synthesized highly bioactive glass–ceramic for bone engineering. They found that the crystalline phase $Na_2Ca_2Si_3O_9$ can transform into an amorphous calcium phosphate phase after immersion in simulated body fluid (SBF) for 28 day.

In the present investigation, the bioactivity behaviour of the crystalline samples $G_3$ and $G_6$ decreased slightly with the $Mg_2SiO_4$/$Na_2Ca_2Si_3O_9$ replacements as indicated from the EDX patterns before and after the soaking in the SBF solution. At low $Mg_2SiO_4$/$Na_2Ca_2Si_3O_9$ replacement, i.e. $G_4$, the decrease of bioactivity may be due to the formation of diopside phase ($CaMgSi_2O_6$) instead of sodium calcium silicate phase ($Na_2Ca_2Si_3O_9$). Nonami et al. [18] investigated the mechanical properties and degradation of the diopside; they showed that diopside-containing ceramics possessed significantly improved mechanical strength when compared with hydroxyapatite and wollastonite ceramics, while the degradation rate of the diopside ceramics was extremely low. The lower value of activation energy means a faster release of Si ions. Wu and Chang [27] found that the activation energy of Si ion release increased and the degradation decreased from bredigite to diopside ceramics with the increase of Mg content, and the apatite-formation ability in SBF decreased.

It is clear that the bioactivity of the studied glass–ceramic sample containing high amount of MgO, (i.e. $G_6$, with 14.32 MgO mole %) was lower than that of sample $G_1$ (MgO-free), as indicated from the EDX patterns (Figs. 7b, 9b, respectively). Figure 9b revealed that the peak for Si was increased, i.e. the surface of $G_6$ sample was not completely covered with apatite layer as compared with that of $G_1$ (Figs. 7a, 9a, respectively). This may be attributed to the increase in the chemical durability of the glass–ceramic materials by increasing the amount of magnesium containing phases like diopside and monticellite ($CaMgSiO_4$). Apatite-formation ability was directly relative to the dissolution of the materials. Following the nucleation and growth mechanisms of apatite formation proposed by Hench, the rate of apatite formation decreases with the decrease of bioglasses dissolution [4]. Previous [28] study showed that Mg in bioglass resulted in a decrease of the solubility of the glass, and one reason is that the higher Mg–O bond energy makes it difficult to release from crystal lattice when compared with the Ca–O bond. In addition, Mg atom in crystal lattice inhibits Ca atom release, which also decreases the solubility of the glass [28]. Wu and Chang [27], prepared three ceramic samples based on Mg containing CaO–$SiO_2$ materials. They reported that with the increase of Mg contents, Mg atom may occupy the position of Ca atom and make the crystal structure more stable because of the higher Mg–O bond energy compared with Ca–O bond and the inhibitory effect of Mg atom on Ca atom release.

The mechanical properties of glass–ceramics, among other variables, depend on volume fraction, grain size, crystal phase and shape of crystals [29]. Glass–ceramics, as fine grained polycrystalline materials prepared by suitable crystallization of special glass system have receiving wide applications for its advantages of high mechanical strength, good abrasion and corrosion resistance [30]. The main reason for development of bioactive glass–ceramics is the desire to produce implant materials with superior mechanical properties to those of the glasses.

The present results revealed that the addition of $Mg_2SiO_4$ at the expense of $Na_2Ca_2Si_3O_9$ in the base glass, increased the microhardness values of the investigated glass–ceramics. This could be attributed to the formation of fine grained microstructure as indicated from the SEM micrograph (e.g. Fig. 10, $G_4$). The microhardness of glass–ceramics generally increased with the increase of the crystallization tendency, smaller crystalline grains as well

as formation of fine microstructure [31]. This may be also due to the formation of relatively higher hardness diopside $CaMgSi_2O_6$ instead of sodium calcium silicate phase (i.e. $G_2$–$G_4$). Among the CaO–MgO–$SiO_2$ system, diopside ceramics are known to have high mechanical strength [18]. Park et al. [32] indicated that glass–ceramics containing large amount of diopside phase generally showed a high microhardness value due to the interlocking microstructures of diopside crystals with microhardness 6,730 MPa. On the other hand, the increase in the amount of diopside phase and the formation of high mechanical strength monticellite ($CaMgSiO_4$) phase may be led to further increase in the microhardness value of glass–ceramic samples ($G_5$ and $G_6$). monticellite is one of the olivine group which is characterized by high hardness [17].

## 5 Conclusions

The crystallization, bioactivity, and microhardness of glass–ceramics based on combeite [$Na_2Ca_2Si_3O_9$]–fluorapatite [$Ca_5(PO_4)_3F$] and forsterite [$Mg_2SiO_4$] system were evaluated. The ICP and EDX analysis demonstrated that a glass–ceramics were covered with HA layer after immersion 3 weeks in SBF solution. Hence the glass–ceramics are bioactive materials. The dissolution of various metal ions and the dynamic changes in pH value were recorded during in vitro dissolution experiments. The pH of the SBF solution and the glass–ceramics degradation were decreased with the increase of $Mg_2SiO_4$ content. The apatite-formation ability was decreased due to the decrease in the solubility of these glass–ceramics. The Vicker's microhardness values (5,047–6,781 MPa) of the obtained glass–ceramic materials were markedly improved by the addition of $Mg_2SiO_4$ due to the crystalline phases formed and grain microstructure developed.

## References


1. Pisciella P, Pelino M. Thermal expansion investigation of iron rich glass–ceramic. J Eur Ceram Soc. 2008;28:3021–6.
2. Peitl O, Zanotto ED, Hench LL. Highly bioactive $P_2O_5$–$Na_2O$–CaO–$SiO_2$ glass–ceramics. J Non-Cryst Solids. 2001;292:115–26.
3. Kim H, Miyaji F, Kokubo T. Bioactivity of $Na_2O$–CaO–$SiO_2$ glasses. J Am Ceram Soc. 1995;78:2405–11.
4. Hench LL. Bioceramics. J Am Ceram Soc. 1998;81:1705–28.
5. Cao W, Hench LL. Bioactive materials. Ceram Int. 1996;22:493–507.
6. Arstila H, Vedel E, Hupa L, Hupa M. Factors affecting crystallization of bioactive glasses. J Eur Ceram Soc. 2007;27:1543.
7. Clupper DC, Mecholsky JJ Jr, Latorre GP, Greenspan DC. Sintering temperature effects on the in vitro bioactive response of tape cast and sintered bioactive glass–ceramic in Tris buffer. J Biomed Mater Res. 2001;57:532–40.
8. Salman SM, Salama SN, Darwish H, Abo-Mosallam HA. In vitro bioactivity of glass–ceramics of the $CaMgSi_2O_6$–$CaSiO_3$–$Ca_5(PO_4)3F$–$Na_2SiO_3$ system with $TiO_2$ or ZnO additives. Ceram Int. 2009;35:1083–93.
9. Clupper DC, Hench LL, Mecholsky JJ. Strength and toughness of tape cast bioactive glass 45S5 following heat-treatment. J Eur Ceram Soc. 2004;24:2929–34.
10. Hench LL, Ethridge EC. Biomaterials: an interfacial approach. New York: Academic Press, Inc.; 1982.
11. Kokubo T, Ito S, Shigematsu M, Sakka S. Mechanical properties of a new type of apatite-containing glass–ceramic for prosthetic application. J Mater Sci Eng. 1985;20:2001–4.
12. Salinas AJ, Roman J, Vallet-Regi M, Oliveira JM, Correia RN, Fernandes MH. In vitro bioactivity of glass and glass ceramics of the $3CaO{\cdot}P_2O_5$–$CaO{\cdot}SiO_2$–$CaO{\cdot}MgO{\cdot}2SiO_2$ system. Biomaterials. 2000;21:251–7.
13. Salama SN, Darwish H, Abo-Mosallam HA. HA forming ability of some glass–ceramics of the $CaMgSi_2O_6$–$Ca_5(PO_4)_3F$–$CaAl_2SiO_6$ system. Ceram Int. 2006;32:357–64.
14. Dietzel A. Z Elektrochem. 1942;48:9–23.
15. Bovo N. Structure—properties relationships in bioactive glasses for PAA—based polyalkenoate cements. Ph.D., Thesis. U.K.: Imperial College London; 2007.
16. Li P, Yang Q, Zhang F. The effect of residual glassy phase in a bioactive glass–ceramic on the formation of its surface apatite layer in vitro. J Mater Sci: Mater Med. 1992;3:452–6.
17. Deer WA, Howie RA, Zussman J. An introduction to the rock-forming minerals. Third ELBS impression. Hong Kong: Common Wealth, Printing Press Ltd.; 1992.
18. Nonami T, Tsutsumi S. Study of diopside ceramics for biomaterials. J Mater Sci: Mater Med. 1999;10:475–7.
19. Ricker RW, Osborn EF. Additional phase-equilibrium data for the system CaO–MgO–$SiO_2$. J Am Ceram Soc. 1954;37:133–9.
20. Roy S, Basu B. In vitro dissolution behavior of $SiO_2$–MgO–$Al_2O_3$–$K_2O$–$B_2O_3$–F glass–ceramic system. J Mater Sci: Mater Med. 2008;19:3123–33.
21. Al-Haidary J, Al-Haidari M, Qrunfuleh S. Effect of yttria addition on mechanical, physical and biological properties of bioactive MgO–CaO–$SiO_2$–$P_2O_5$–$CaF_2$ glass ceramic. Biomed Mater. 2008;3:015005 (5pp).
22. Hench LL, West J. Biological applications of bioactive glasses. Life Chem Rep. 1996;13:187.
23. Paul A. Chemistry of glasses. London: Chapman & Hall; 1982.
24. Oliveira JM, Correia RN, Fernandes MH. Effects of Si speciation on the in vitro bioactivity of glasses. Biomaterials. 2002;23:371–9.
25. Oliveira JM, Correia RN, Fernandes MH. Surface modification of a glass and a glass–ceramic of the MgO–$3CaO{\cdot}P_2O_5$–$SiO_2$ system in a simulated body fluid. Biomaterials. 1995;16:849–54.
26. Chen QZ, Thompson ID, Boccaccini AR. 45S5 Bioglass®-derived glass–ceramic scaffolds for bone tissue engineering. Biomaterials. 2006;27:2414–25.
27. Wu C, Chang J. Degradation, bioactivity, and cytocompatibility of diopside, akermanite, and bredigite ceramics. J Biomed Mater Res B: Appl Biomater. 2007;83B:153–60.
28. Vallet-Regi V, Salinas AJ, Roman J, Gil M. Effect of magnesium content on the in vitro bioactivity of CaO–MgO–$SiO_2$–$P_2O_5$ sol–gel glasses. J Mater Chem. 1999;9:515–8.
29. Höland W, Beall GH. Glass–ceramic technology. Westerville, OH: Am. Ceram. Soc., Inc.; 2002.
30. Sevim I, Kulekci M. Abrasive wear behavior of bioactive glass–ceramics containing apatite. Bull Mater Sci. 2006;29:243–9.
31. Torres FJ, Alarcon J. Mechanism of crystallization of pyroxene based glass–ceramic glazes. J Non-Cryst Solids. 2004;347:45–51.
32. Park YJ, Moon SO, Heo J. Crystalline phase control of glass–ceramics obtained from sewage sludge fly ash. Ceram Int. 2003;29:223–7.